INTERNATIONAL
ATOMIC ENERGY
AGENCY

UNITED NATIONS
EDUCATIONAL,
SCIENTIFIC
AND CULTURAL
ORGANIZATION

LAMP/91/9

INTERNATIONAL CENTRE FOR
THEORETICAL PHYSICS

LAMP
SERIES REPORT

(Laser, Atomic and Molecular Physics)

HYPER-RAMAN SCATTERING AND THREE-PHOTON RESONANT IONIZATION: COMPETITIVE EFFECTS

A.M. Guzmán

and

C. Ramírez

MIRAMARE-TRIESTE

International Atomic Energy Agency

and

United Nations Educational Scientific and Cultural Organization

INTERNATIONAL CENTRE FOR THEORETICAL PHYSICS

LAMP SERIES REPORT

(Laser, Atomic and Molecular Physics)

HYPER-RAMAN SCATTERING AND THREE-PHOTON RESONANT IONIZATION: COMPETITIVE EFFECTS

A.M. Guzmán *

International Centre for Theoretical Physics, Trieste, Italy

and

C. Ramírez

Departamento de Física, Universidad Nacional de Colombia, Bogotá, Colombia.

ABSTRACT

A semiclassical theory of hyper–Raman scattering and three–photon resonant ionization via the coupled density–matrix and Maxwell equations is presented. A simplified three–level atom model is obtained, which includes two–photon resonant pumping and time dependent photoionization rates. We consider conditions typically encountered in atomic vapours to simulate numerically pulse propagation. A strong depletion of the photoionization probability in the hyper–Raman field saturation regime is predicted.

MIRAMARE – TRIESTE

September 1991

* Permanent address: Departamento de Física, Universidad Nacional de Colombia, Bogotá, Colombia.

Preface

The ICTP-LAMP reports consist of manuscripts relevant to seminars and discussions held at ICTP in the field of Laser, Atomic and Molecular Physics (LAMP).

These reports aim at informing LAMP researchers on the activity carried out at ICTP in their field of interest, with the specific purpose of stimulating scientific contacts and collaboration of physicists from Third World Countries.

If you are interested in receiving additional information on the Laser and Optical Fibre activities at ICTP, kindly contact Professor Gallieno Denardo, ICTP.

1 Introduction

Recently, the study of competitive nonlinear effects has been object of considerable work[1-6]. Several experimental and theoretical studies have shown interference effects leading to suppression of hyper-Raman Scattering (HRS) by four-wave mixing (FWM)[1,2], or competition between multiphoton ionization and third-harmonic generation[3,6]. In this paper, we introduce the three-photon resonant ionization (TPRI) as an alternate channel to HRS in a nonlinear vapor. Simultaneous measurements of TPRI probability, and fluorescence from the resonant level have been performed[7], but to our knowledge, experimental analysis of competitive effects in a nonlinear amplifier have not been reported.

In Sections **2** and **3**, we give the formal development of the theory. We describe the fields classically and the medium quantum mechanically via its density-matrix. We consider a whole set of bound and continuum atomic states, and derive an atom-field model, which retains the simplicity of a three-level system, but includes the effect of the positive-energy continuum states through time dependent ionization rates. The equations of motion for the elements of the density-matrix are obtained by elimination of nonresonant and continuum states. The procedure leads to a set of three-level system equations with an effective two-photon transition probability, which includes population and phase relaxation rates related to ionization.

In section **3**, we perform the slowly varying amplitude and phase approximation and obtain the field equations. In Section **4**, we solve numerically the coupled density-matrix and Maxwell equations, and describe the atomic dynamics as well as HRS and TPRI along the medium. As a result of the strong saturation of the HRS, competitive effects leading to a strong depletion of the TPRI probability are found. Further discussion and conclusions are given in Section **5**.

2 Density-matrix equations

We consider a homogeneously broadened atomic system with three active levels, a set $\{|i>\}$ of bound nonresonant levels, and a continuum of states $|\omega>$ (Figure 1). Under conditions of two-photon resonant interaction of an atomic vapor with a laser field of frequency ν_1, radiation of frequency ν_2 is

generated by HRS, and TPRI to the continuum takes place by the absorption of three fundamental laser photons.

Density matrix equations for a two-photon pumped three-level system in absence of ionization were obtained in a previous paper[8] by adiabatic elimination of the nonresonant set of bound intermediate levels, which jointly with the state $|3>$ determine the two-photon transition probability[9,10]. Here we extend the model to include the coupling to the positive-energy continuum states $|\omega>$ by the method proposed in references[11,12].

We consider linearly polarized fields propagating along $\mathbf{z}$, and express the total electric field as

$$\mathbf{E}(z,t) = \frac{1}{2}\mathbf{u}\sum_{\alpha=1}^{2}[\mathcal{E}_\alpha(z,t)\exp[i(k_\alpha z - \nu_\alpha t)] + c.c.], \tag{1}$$

where the complex amplitudes $\mathcal{E}_\alpha(z,t)$ are assumed to be slowly varying.

The density-matrix operator obeys the Liouville equation

$$\frac{\partial\rho}{\partial t} = -\frac{i}{\hbar}[H,\rho] + \dot{\rho}_R \tag{2}$$

where H is the atomic Hamiltonian in the electric dipole approximation, and $\dot{\rho}_R$ stands for population and phase relaxation processes.

As in reference [8], we expand the bound-bound density-matrix elements in the Fourier series:

$$\rho_{mj}(z,t) = \sum_{NL}\sigma_{mj}^{NL}(z,t)\exp[i(\nu_{NL}t - k_{NL}z)] \tag{3}$$

where σ_{mj}^{NL} are slowly varying amplitudes, $\nu_{NL} = N\nu_1 + L\nu_2$, and $k_{NL} = Nk_1 + Lk_2$.

The interaction picture is completed by assuming

$$\begin{aligned}
\rho_{1\omega}(z,t) &= \sigma_{1\omega}(z,t)\exp[3i(\nu_1 t - k_1 z)] \\
\rho_{2\omega}(z,t) &= \sigma_{2\omega}(z,t)\exp i(\nu_1 t - k_1 z) \\
\rho_{3\omega}(z,t) &= \sigma_{3\omega}(z,t)\exp i[(\nu_1+\nu_2)t - (k_1+k_2)z]
\end{aligned} \tag{4}$$

By replacing (1), (3), and (4) into (2), equations for the amplitudes σ_{mj}^{NL} and $\sigma_{j\omega}$ are obtained. For given m, and j, there is one near-resonant amplitude in equation (3), which satisfies

$$\omega_{mj} + \nu_{NL} \sim 0, \tag{5}$$

where $\hbar\omega_{mj}$ is the energy difference between the states $|m>$ and $|j>$. The nonresonant amplitudes can be adiabatically eliminated whenever the condition

$$|\frac{\partial \mathcal{E}_1}{\partial t}| \ll |(\omega_{mj} + \nu_{NL})\mathcal{E}_1| \tag{6}$$

is fulfilled[13]. We ignore the coupling between nonresonant amplitudes as well as between continuum-bound density-matrix elements, and apply the rotating wave approximation. Then to first order in $\mathcal{E}_2$ we obtain[1]

$$\dot{\sigma}_{11} = \Gamma_3\sigma_{33} + (i\sigma_{12}V_{21} + c.c.) \tag{7}$$

$$\dot{\sigma}_{22} = -\Gamma_2\sigma_{22} - (i\sigma_{12}V_{21} + i\sigma_{32}V_{23} + \frac{i}{2\hbar}\int_0^\infty d\omega\ \wp_{\omega 2}\sigma_{2\omega}\mathcal{E}_1 + c.c.) \tag{8}$$

$$\dot{\sigma}_{33} = -\Gamma_3\sigma_{33} + \Gamma_2\sigma_{22} + (i\sigma_{32}V_{23} + c.c.) \tag{9}$$

$$\dot{\sigma}_{\omega\omega} = 0 \tag{10}$$

$$\dot{\sigma}_{21} = -(\Gamma_{21} + i\Delta_1 + i\delta_{21})\sigma_{21} - i\sigma_{31}V_{23} + iV_{21}(\sigma_{22} - \sigma_{11}) + \frac{i}{2\hbar}\int_0^\infty d\omega\ \wp_{2\omega}\sigma_{\omega 1}\mathcal{E}_1^* \tag{11}$$

$$\dot{\sigma}_{23} = -(\Gamma_{23} + i\Delta_2 + i\delta_{23})\sigma_{23} - i\sigma_{13}V_{21} + iV_{23}(\sigma_{22} - \sigma_{33}) + \frac{i}{2\hbar}\int_0^\infty d\omega\ \wp_{2\omega}\sigma_{\omega 3}\mathcal{E}_1^* \tag{12}$$

$$\dot{\sigma}_{13} = -(\Gamma_{13} - i\Delta_3 + i\delta_{13})\sigma_{13} + (i\sigma_{12}V_{23} - i\sigma_{23}V_{12}) \tag{13}$$

$$\dot{\sigma}_{1\omega} = i(\omega - \omega_e)\sigma_{1\omega} - (\frac{i}{2\hbar})\wp_{2\omega}\sigma_{12}\mathcal{E}_1^* \tag{14}$$

$$\dot{\sigma}_{2\omega} = i(\omega - \omega_e - \Delta_1)\sigma_{2\omega} - (\frac{i}{2\hbar})\wp_{2\omega}\sigma_{22}\mathcal{E}_1^* \tag{15}$$

$$\dot{\sigma}_{3\omega} = i(\omega - \omega_e - \Delta_3)\sigma_{3\omega} - (\frac{i}{2\hbar})\wp_{2\omega}\sigma_{32}\mathcal{E}_1^* \tag{16}$$

where the dot means partial time derivative. $\wp$ is the component of the atomic dipole operator along the polarization axis $\mathbf{u}$. $\Gamma_j, j = 2,3$ and Γ_{mj}, $m \neq j$ stand for spontaneous decay and collisional phase relaxation rates respectively; $\Delta_1 = \omega_{21} - 2\nu_1, \Delta_2 = \omega_{23} - \nu_2, \Delta_3 = \omega_{31} - \nu_3, \omega_e = \omega_1 + 3\nu_1$. Conservation of energy implies $2\nu_1 = \nu_2 + \nu_3$ and $\Delta_1 = \Delta_2 + \Delta_3$. The ac Stark shifts are defined as $\delta_{mk} =: \delta_m - \delta_k, m,k = 1,2,3,4$, with

$$\delta_m = -(\frac{1}{2\hbar})^2 \sum_j \frac{|\wp_{mj}|^2\omega_{jm}|\mathcal{E}_1|^2}{(\omega_{jm}^2 - \nu_1^2)}, \tag{17}$$

[1]For simplicity, the superscripts NL will be omitted in the following.

where summation includes the four active levels and all other intermediate bound or continuum levels. The reduced matrix elements of the interaction Hamiltonian are given by

$$V_{21} = \frac{k_{21}\mathcal{E}_1^2}{2\hbar}, \qquad V_{23} = -\frac{\wp_{23}\mathcal{E}_2}{2\hbar}, \tag{18}$$

where

$$k_{21} = -\frac{1}{2\hbar}\sum_j \frac{\wp_{2j}\wp_{j1}}{(\omega_{2j} - \nu_1)}\ , \tag{19}$$

plays the role of an effective two-photon coupling constant. Formal integration of $\dot{\sigma}_{2\omega}$ of equation (15) and substitution in (8) lead to

$$\dot{\sigma}_{22} = -\Gamma_2\sigma_{22} - (i\sigma_{12}V_{21} + i\sigma_{32}V_{23} + c.c.) - \frac{1}{2\hbar^2}\int_0^\infty d\omega\ \wp_{2\omega}^2\int_0^t d\tau\ \sigma_{22}(t-\tau)\mathcal{E}_1^*(t-\tau)\mathcal{E}_1(t) \times \exp[i(\omega - \omega_e - \Delta_1)]\tau \tag{20}$$

The integral over ω can be easily done by assuming a fictitious Lorentzian distribution for the square dipole transition matrix elements $|\wp_{2\omega}|^2$ centered at ω_B (Figure 1), whose width B is much larger than $\omega_B - \omega_e$, and than the laser linewidth[11]. In order to perform the time integral, we further assume that σ_{22}, and the field amplitude $\mathcal{E}_1(t)$ are slowly varying in the time scale of B^{-1}, and obtain

$$\dot{\sigma}_{22} = -(\Gamma_2 + \Gamma_I(t))\sigma_{22} - (i\sigma_{12}V_{21} + i\sigma_{32}V_{23} + c.c.) \tag{21}$$

The same procedure applied to equations (11) and (12) leads to the completion of a simple two-photon three-level model[8]. The continuum states are eliminated, but their influence is retained through population and phase relaxation rates due to photoionization:

$$\dot{\sigma}_{21} = -(\Gamma_{21} + \frac{\Gamma_I(t)}{2} + i\Delta_1 + i\delta_{21})\sigma_{21} - i\sigma_{31}V_{23} + iV_{21}(\sigma_{22} - \sigma_{11}) \tag{22}$$

$$\dot{\sigma}_{23} = -(\Gamma_{23} + \frac{\Gamma_I(t)}{2} + i\Delta_2 + i\delta_{23})\sigma_{23} - i\sigma_{13}V_{21} + iV_{23}(\sigma_{22} - \sigma_{33}) \tag{23}$$

Equations (7), (9), and (13) remain unchanged. The time dependent photoionization rate

$$\Gamma_I(t) = \frac{\pi}{2\hbar^2}\wp_{2\omega_e}^2|\mathcal{E}_1(t)|^2 \tag{24}$$

coincides with the one-photon ionization rate from state $|2>$ into the continuum, and is proportional to both, the ionization cross section and the photon flux at time t. It can also be expressed as $\Gamma_I(t) = \Gamma_{I0}|V_{21}(t)|$, where

$$\Gamma_{I0} =: \frac{\pi\wp_{2\omega_e}^2}{\hbar k_{21}}. \tag{25}$$

3 Field equations

In analogy to equation (1) we express the total polarization in the medium as:

$$\mathbf{P}(z,t) = \frac{1}{2}\mathbf{u}\sum_{\alpha=1}^{2}[\mathcal{P}_\alpha(z,t)\exp[i(k_\alpha z - \nu_\alpha t)] + c.c.], \tag{26}$$

where $\mathcal{P}_\alpha(z,t)$ are slowly varying complex amplitudes. It is explicitly given by

$$\mathbf{P}(z,t) = NTr(\rho\wp) \tag{27}$$

where N is the atomic density. Replacing equations (1), (3), (26), and (27) into the wave equation, and applying the slowly varying approximation we obtain

$$\frac{\partial\mathcal{E}_\alpha}{\partial z} + \frac{1}{v_\alpha}\frac{\partial\mathcal{E}_\alpha}{\partial t} = \frac{ik_\alpha}{2\epsilon_\alpha}\mathcal{P}_\alpha^{res}, \quad \alpha = 1,2, \tag{28}$$

where

$$\begin{aligned}\mathcal{P}_1^{res} &= -4Nk_{21}\sigma_{21}\mathcal{E}_1^* \\ \mathcal{P}_2^{res} &= 2N\wp_{32}\sigma_{23},\end{aligned} \tag{29}$$

and ϵ_α is the dielectric constant of the medium at frequency ν_α. The nonresonant elements determine the linear susceptibility and hence the phase velocity $\mathbf{v}_\alpha$ of the wave in the medium. The term leading to nonresonant absorption has been ignored.

4 Pulse propagation

In this Section, we present the results of the numerical solution of the coupled density-matrix and Maxwell equations. For simplicity and from experimental evidence[13] we neglect pump depletion. Since only forward waves are considered, it is convenient to introduce the retarded time $\tau = t - z/v_2 \mathrm{W}\tau = t - z/v_2$ and $\zeta = z$. Then, in terms of the reduced interaction matrix element V_{23}, the HRS field equation becomes

$$\frac{\partial V_{23}}{\partial\zeta} = -iA_2\sigma_{23}, \qquad A_2 = \frac{k_2 N}{2\hbar\epsilon_2}|\wp_{23}|^2 \tag{30}$$

The incident driving field is taken to be real and Gaussian:

$$V_{21} = V_{21}^{max}\exp[-\frac{(\tau-\tau_0)^2}{\tau_P^2}], \tag{31}$$

and the initial HRS field is taken as a small constant.

We take the atomic system to be in its ground state at $\tau = 0$, i.e., we assume swept excitation. The integration is performed by solving the density-matrix equations for all times for successive slices of the amplifier. The values of the atomic parameters involved in the calculations have been evaluated for the specific case of the two-photon transition $3S_{\frac{1}{2}} - 7S_{\frac{1}{2}}$ in Na. Bound-bound dipole matrix elements were calculated by the Bates and Daamgard approach[14], and Γ_{I0} was obtained from analytical expressions given in the literature[15]. The pump pulse has been chosen to be centered at $\tau_0 = 9nsec$, and to have a width of $6nsec$ and an amplitude roughly correspondent to a pump intensity of $5 \times 10^7 Watt/cm^2$. All calculations have been done for $A_2 = 200cm^{-1}$, which corresponds to an atomic density of $10^{15}at/cm^3$, and for $\Delta_2 = 0$. We have assumed small phase relaxation rates (consistent with the low density of Na vapor) to retain coherent effects. AC Stark shifts were included, and most of the curves presented correspond to detuned pumping at roughly the effective Stark shifted resonance.

In Figure 2, the temporal behavior of the populations on the three active levels for various amplifier lengths is shown. At $z = 0$ (Figure 2a), the system behaves essentially as a two-photon pumped two-level system (levels $|1>$ and $|2>$ in Figure 1) undergoing Rabi oscillations, and the population in level $|3>$ is negligible. The population inversion between levels $|2>$ and

$|3>$ gives rise to stimulated HRS. As the HRS field becomes amplified in the medium (Figures 2b-2d), the atomic dynamics is strongly modified.The HRS field couples to the transition $|2> \leftrightarrow |3>$, and induces Rabi oscillations between those levels.

The amplification process of the HRS pulse along the vapor can be seen in Figure 3. There the pulse intensity is represented as function of both, the effective medium length Nz and time. Its temporal oscillations are related to those of populations.

The photoionization probability is obtained from the dynamical evolution of level populations. It can be characterized by a time dependent relative ionization rate

$$\alpha(t) = -\frac{1}{\sigma_T}\frac{\partial \sigma_T}{\partial t} \tag{32}$$

where σ_T is the total population. From the density-matrix equations we obtain

$$\alpha(t) = \frac{\Gamma_I(t)\sigma_{22}(t)}{\sigma_T(t)}, \tag{33}$$

which means that its temporal behavior is essentially determined by that of σ_{22}. A strong reduction of $\alpha(t)$ as function of the effective medium length is observed in Figure 4. The correlation with the growth of the HRS field is evident (see Figure 8). The HRS field contributes to trap population through its coherent interaction with the $|2> \leftrightarrow |3>$ transition, and suppress ionization.

The tuning characteristics of the hyper-Raman field and photoionization probability have been also analyzed. In Figure 5 we show the HRS output pulse one would obtain at a fixed amplifier length, for different pump pulse detunings. Since we have considered AC Stark shifts, the maximum corresponds to detuned pumping at roughly the Stark shifted resonance, around $\Delta_1 = -13.5 nsec^{-1}$. There is an asymmetry with respect to the maximum, which would not be observed if AC Stark shifts were not present. Calculations done by setting arbitrarily all AC Stark shifts to zero do not show such asymmetry.

The other quantities relevant to our analysis are the HRS field energy, and the ionization probability at the end of the pulse evaluated as $1 - \sigma_T$, when the pulse is over. Both quantities are shown in Figure 6 as function of the pump detuning Δ_1, and for a fixed amplifier length. Oscillations in both curves coincide since the resonant behavior of both processes is essentially

determined by that of population in level $|2>$. The asymmetry due to the AC Stark shift is clearly seen.

Competitive effects between both processes are better observed in Figs. 7 and 8. In obtaining these curves we have arbitrarily set all AC Stark shifts to zero. This simplification allows to distinguish effects due to sweeping of the two-photon pumping rates from those due to the AC Stark shift modulation. In Figure 7, the HRS field energy is shown as function of the z coordinate of the amplifier. The onset of the HRS saturation regime takes place at a threshold value, which lays around $z = 0.1$ for resonant pumping, and increases with the pump detuning. When competitive effects are non relevant, the saturation regime is linear in z[13,16]. Its nonlinear behavior is due to competition with the ionization process, and has also been obtained for competition between HRS and VUV generation by FWM[17]. Finally, the ionization probability at the end of the pulse as function of z is shown in Fig. 8. It remains constant until the onset of the HRS saturation regime, and thereafter it decreases by as much as 80% for resonant pumping. Detuned pumping shifts the onset of the HRS saturation regime to longer effective medium lengths.

5 Summary and conclusions

We have presented results for competitive effects between HRS and TPRI arising from propagation effects through a nonlinear vapor. For thin samples, the dynamics of the atomic system , and hence the HRS gain and the TPRI probability, is mainly determined by the two-photon Rabi flopping induced by the resonant pump field. In this regime, the fluorescence from the resonant level has not remarkable effect on TPRI, since it takes place in a different time scale. Nevertheless, stimulated processes like HRS can become determinant of the atomic dynamics. Because of the stimulated emission to level $|3>$, a two-level model of TPRI is not appropriate in this case.

From the analysis of the temporal and spatial behavior of both, the populations and the HRS pulse, we conclude that saturation of the $|2> \leftrightarrow |3>$ transition leads to population trapping on those levels and then to suppression of TPRI. On its turn, TPRI alters the linear dependence of HRS on density in its saturation regime. These competitive effects cannot be inferred from treatments which not take in account propagation through the medium. Rather, it is necessary to solve the complete set of coupled density-matrix and Maxwell equations along the amplifier. These results also suggest the great importance that alternate dynamic channels can have in nonlinear processes taking place in extense mediums.

ACKNOWLEDGMENTS

One of the authors (A.M.G.) would like to thank Professor Abdus Salam, the International Atomic Energy Agency and UNESCO for hospitality at the International Centre for Theoretical Physics, Trieste.

References

1. Yu P. Malakyan, Opt. Commun. **69**, 315 (1989).

2. M. A. Moore, W. R. Garrett and M. G. Payne, Opt. Commun. **68**, 310 (1988).

3. J. C. Miller, R. N. Compton, M. G. Payne and W. W. Garrett, Phys. Rev. Lett. **45**, 114 (1980); J. C. Miller and R. N. Compton, Phys. Rev. **A25**, 2056 (1982).

4. D. J. Jackson, J. J. Wynne, and P. H. Kes, Phys. Rev. **A28** , 781 (1983).

5. M. Poirier, Phys. Rev. **A27**, 934 (1983); M. G. Payne, W. R. Garret, Phys. Rev. **A28**, 3409 (1983).

6. M. Elk, P. Lambropoulos, and X. Tang, Phys. Rev **A44**, R31 (1991).

7. C. C. Wang, J. V. James, J. V. Xia, in *"LASER SPECTROSCOPY VI"*, ed. H. P. Weber and W. Lüthy, Springer Verlag, p.356 (1983).

8. A. Guzmán de García, P. Meystre, and R. R. E. Salomaa, Phys. Rev. **A32**, 1531 (1985).

9. M. Göppert-Mayer, Ann. Phys. (Leipz) **9**, 273 (1931).

10. M. Takatsuji, Phys. Rev. **A11**, 619 (1975); D. Grischkowsky, M. M. Loy, and P. F. Liao, Phys. Rev. **A12**, 251 (1975).

11. J. L. F. de Meijere and J. H. Eberly, Phys. Rev. **A27**, 1416 (1978).

12. J. H. Eberly, Phys. Rev. Lett. **42**, 1049 (1979).

13. A. Guzmán, "Nonlinear Processes in two-photon pumped atomic vapors", Max Planck Institut for Quantum Optics, Garching, Germany. - Report **91** (1984).

14. J. Heinreich. Dissertation, Universität Düsseldorf (1983).

15. D. R. Bates and A. Damgaard, Phil. Trans. Roy. Soc. London **A242**, 101 (1949).

16. A. Burguess and M. Seaton, Rev. Mod. Phys. **30**, 992 (1958).

17. A. Guzmán, Rev. Acad. Colom. Cienc. **17**, 567 (1990).

Figure captions

Figure 1. Level scheme with the laser field coupling levels $|1>$, $|2>$ and the continuum states $|\omega>$. Stimulated HRS takes place from level $|2>$ to level $|3>$. A non realistic Lorentzian frequency dependence for $|\varphi_{2\omega}|^2$ is shown.

Figure 2. Populations in the active levels as function of time for (a) $z = 0$, (b) $z = 0.128cm^{-1}$, (c) $z = 0.174cm^{-1}$, (d) $z = 0.205cm^{-1}$, and $N = 10^{15}cm^{-3}$. Other values used in the calculation are $|V_{21}^{max}| = 1.21nsec^{-1}, \Delta_1 = -13.5nsec^{-1}, \Delta_2 = 0, \Gamma_2 = 0.06nsec^{-1}, \Gamma_3 = 1.4nsec^{-1}, \Gamma_{I0} = 0.003nsec^{-1}$, $\Gamma_{21} = 0.9nsec^{-1}, \Gamma_{13} = 0.9nsec^{-1}, and \Gamma_{23} = 1nsec^{-1}$.

Figure 3. Hyper-Raman field intensity as function of both, the effective amplifier length and time. All parameters like in Figure 2.

Figure 4. Relative ionization rate as function of both, the effective amplifier length and time. All parameters like in Figure 2.

Figure 5. Hyper-Raman field intensity as function of both, the pump detuning Δ_1 and time, at $z = 0.4cm$. All other parameters like in Figure 2.

Figure 6. Hyper-Raman field energy (dashed line) and photoionization probability (full line) at the end of the pulse as function of the pump detuning Δ_1. The Stark shifted resonance lays around $\Delta_1 = -13.5nsec^{-1}$

Figure 7. Hyper-Raman field energy as function of the effective amplifier length for $\Delta_2 = 0$, and $\Delta_1 = 0$ (full line), $\pm 1nsec^{-1}$(dashed line), $\pm 2nsec^{-1}$ (dot-dashed line). For simplicity AC Stark shifts were arbitrarily set to zero.

Figure 8. Photoionization probability at the end of the pump pulse as function of the effective amplifier length for $\Delta_1 = 0$ (full line), $\pm 1nsec^{-1}$(dashed line), $\pm 2nsec^{-1}$ (dot-dashed line). Other parameters like in Figure 7.

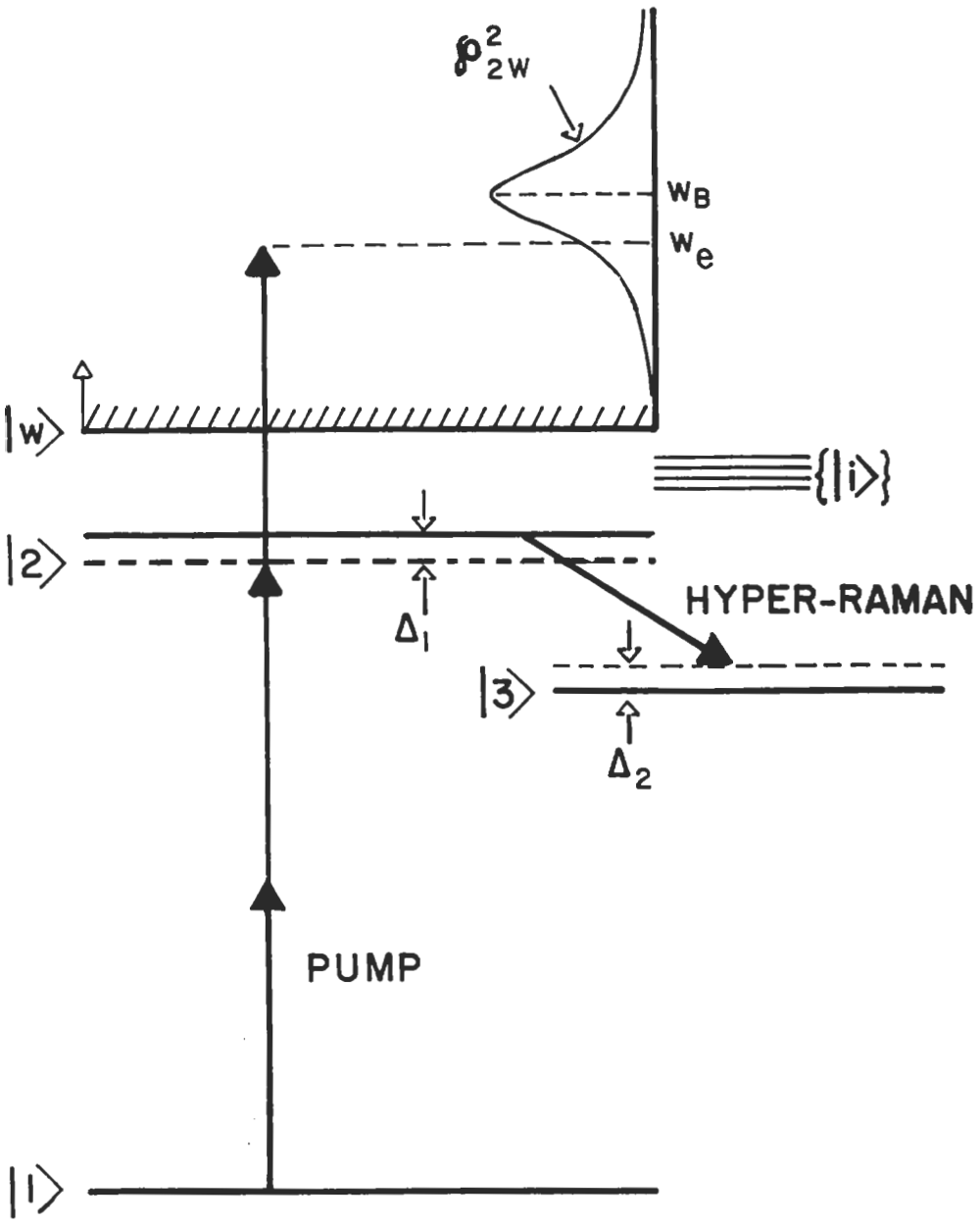
ρ^2_{2w}
w_B
w_e
|w⟩
{|i⟩}
|2⟩
Δ_1
HYPER-RAMAN
|3⟩
Δ_2
PUMP
|1⟩

Fig.1

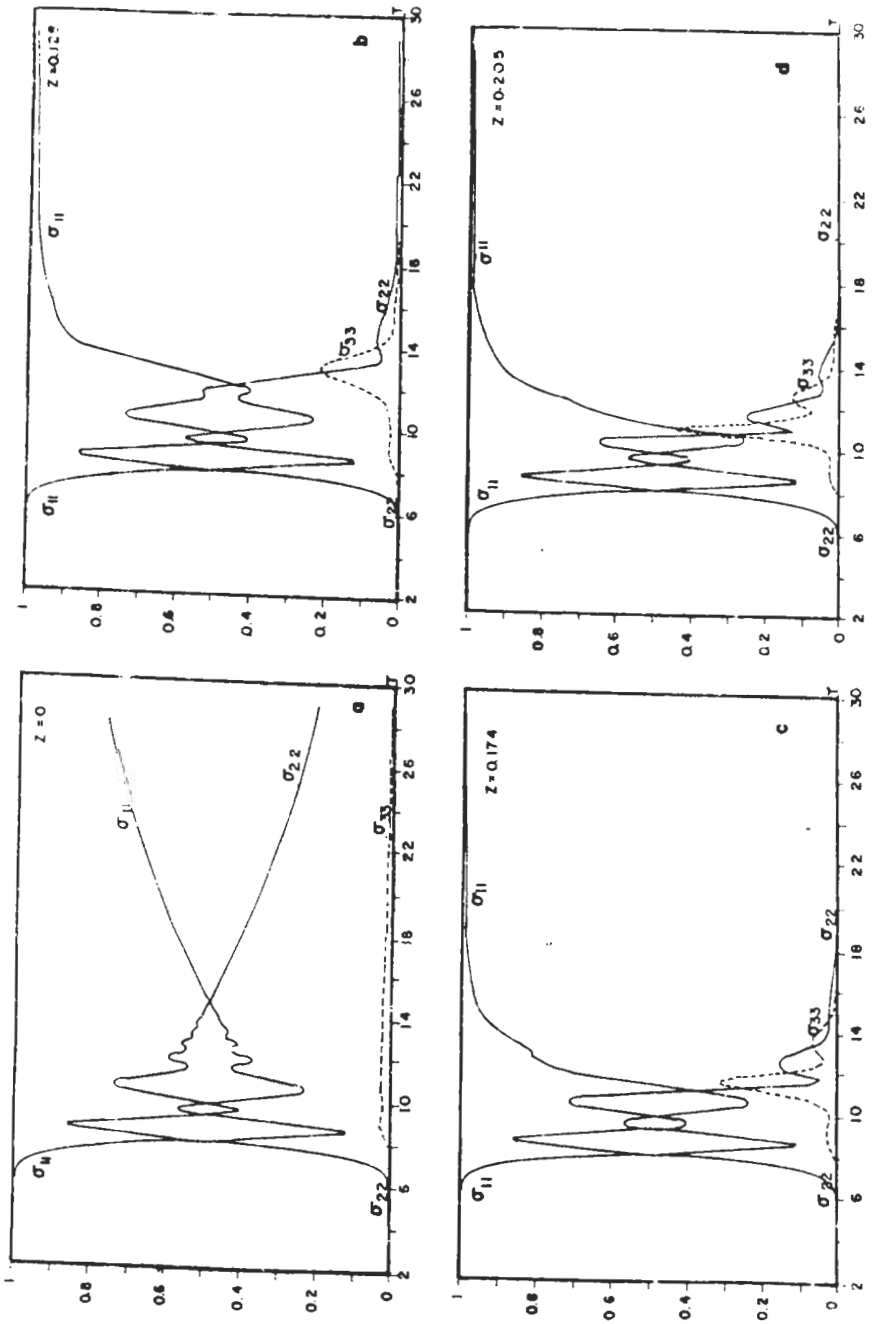
b
Z=0.129
d
Z=0.205
a
Z=0
c
Z=0.174

Fig.2

HYPER-RAMAN FIELD

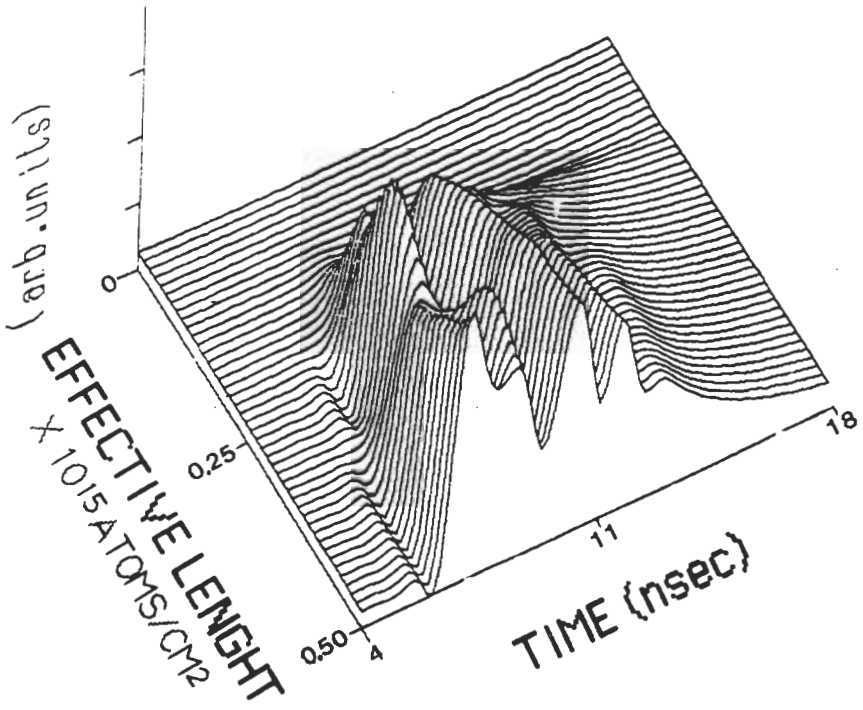

Fig.3

RELATIVE IONIZATION RATE

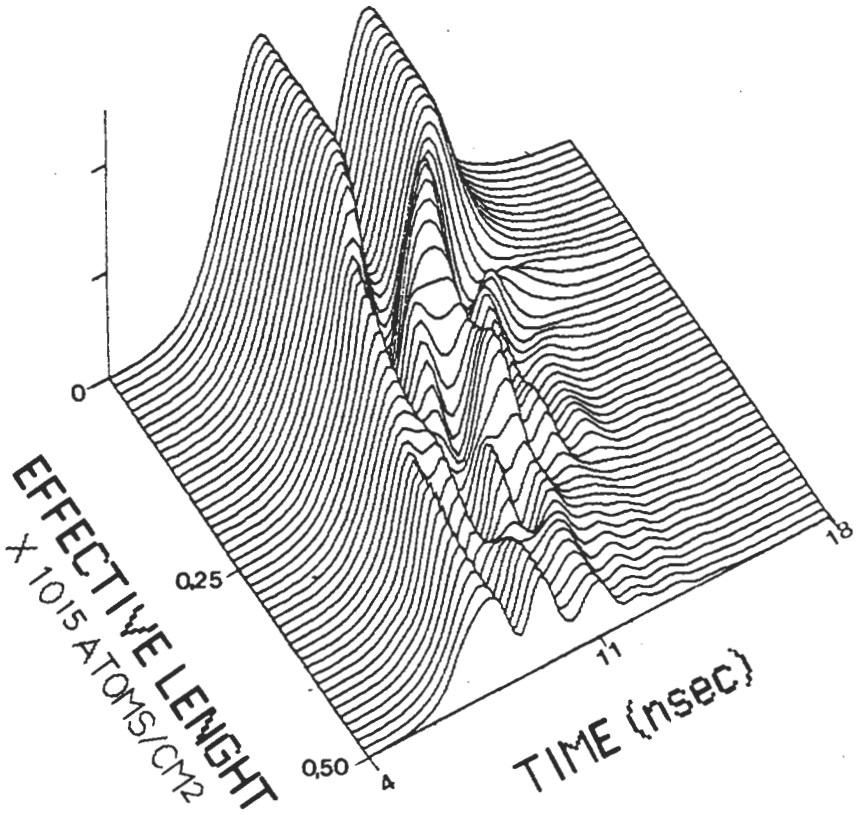

Fig.4

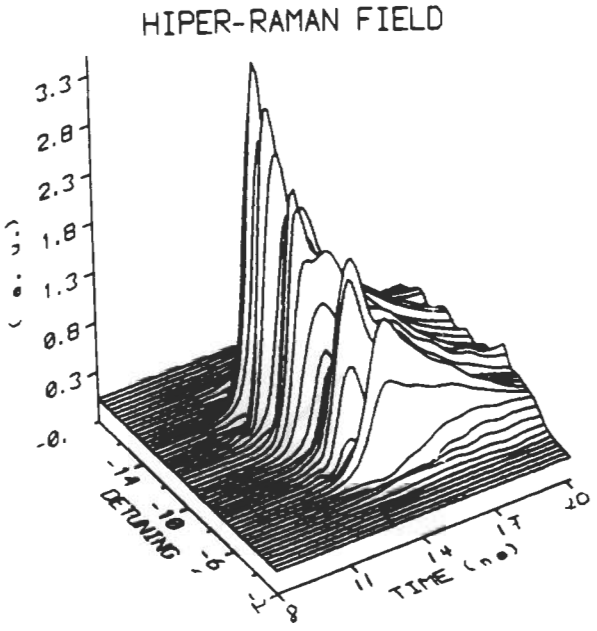
HIPER-RAMAN FIELD
3.3
2.8
2.3
1.8
1.3
0.8
0.3
-0.
DETUNING
TIME (nse)

Fig.5

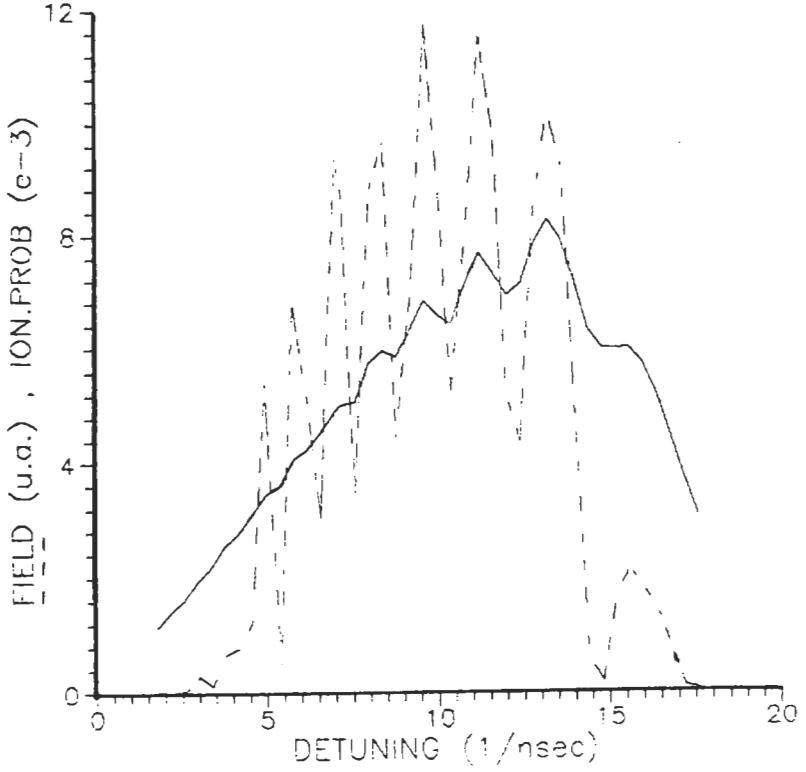
12
8
4
0
FIELD (u.a.) , ION.PROB (e-3)
0
5
10
15
20
DETUNING (1/nsec)

Fig.6

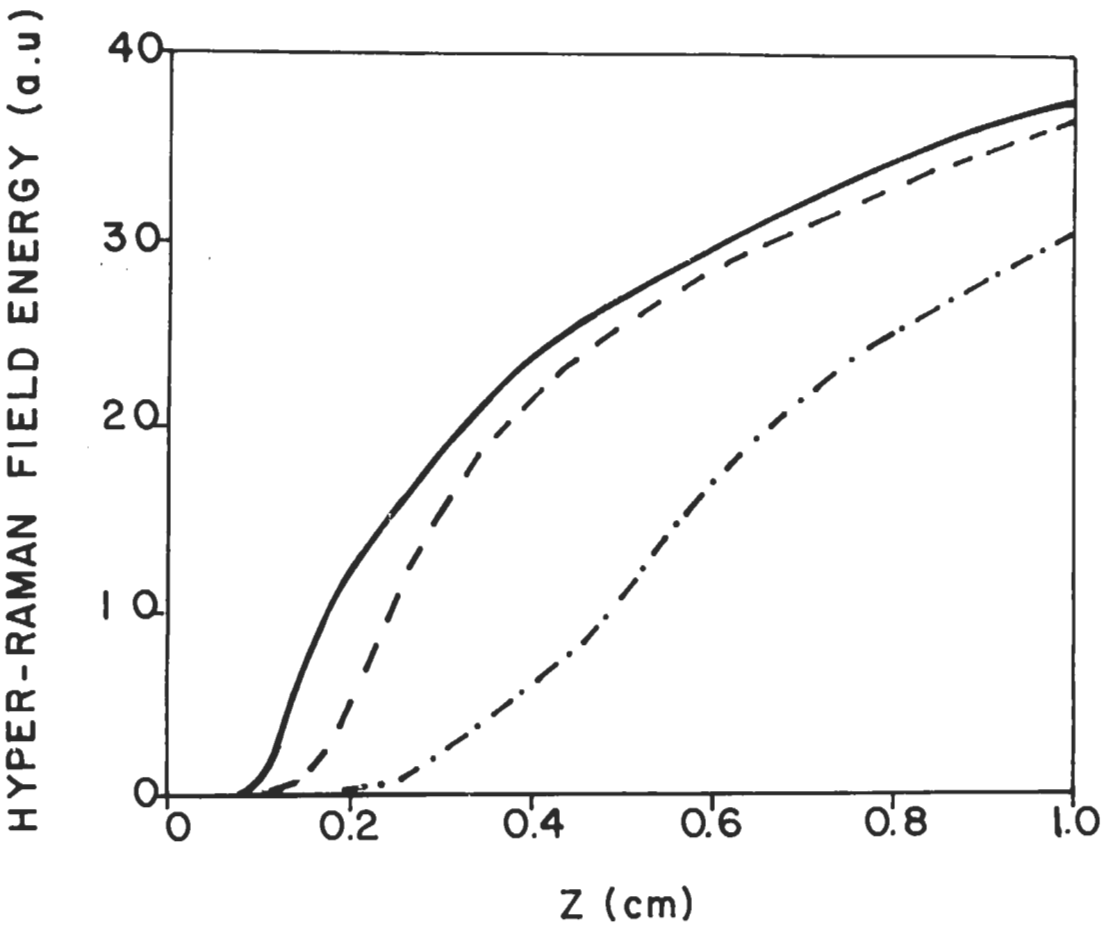
HYPER-RAMAN FIELD ENERGY (a.u)
40
30
20
10
0
0
0.2
0.4
0.6
0.8
1.0
Z (cm)

Fig.7

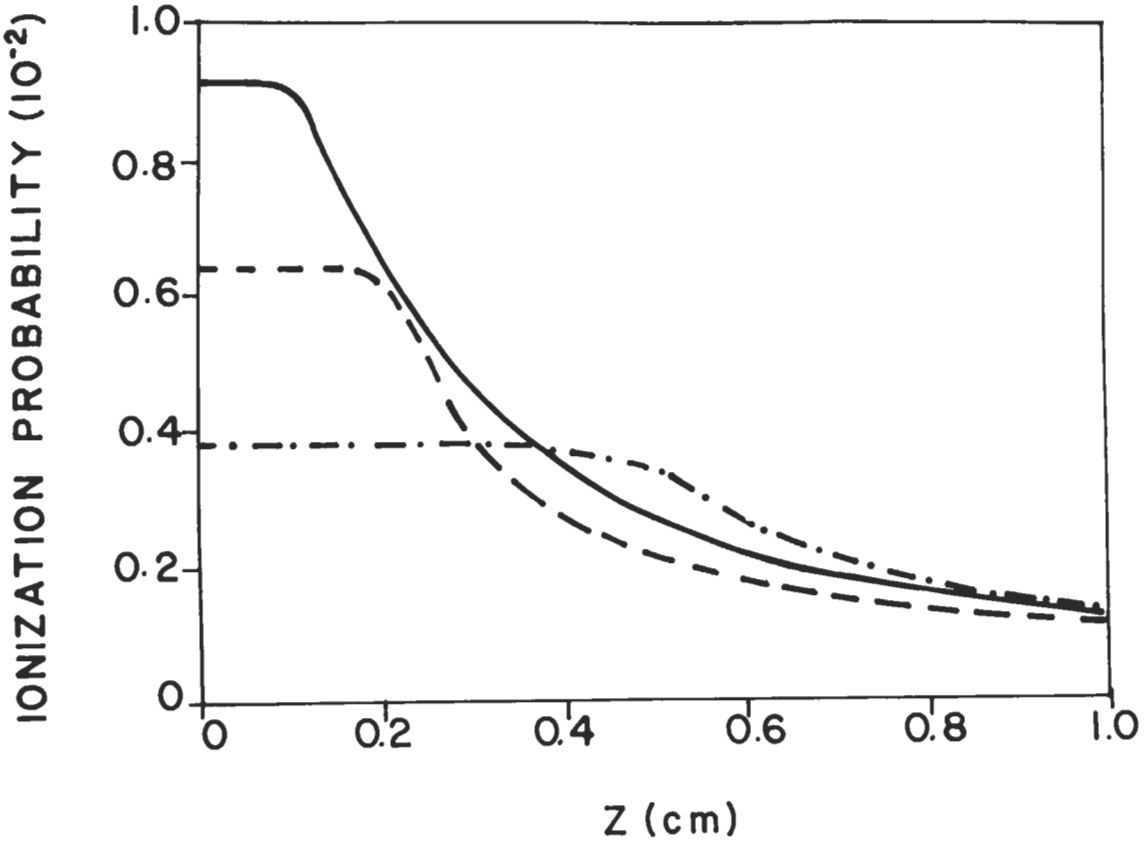
IONIZATION PROBABILITY (10⁻²)
1.0
0.8
0.6
0.4
0.2
0
0
0.2
0.4
0.6
0.8
1.0
Z (cm)

Fig.8